Modelling and Analysis of Three-degree of Freedom Micro-positioning Stage

U.Sudhakar, J.Srinivas

Abstract

This paper presents a design and analysis approach for micropositioning stage based on 3-RPR parallel kinematic linkage. The dimensions of the stage are first obtained and static, dynamic characteristics of the stage are predicted. The objective here is to maximize the workspace (for ranges of both position and orientation) and minimize the singularities inherent in the system. After arriving the dimensions, the finite element model of linkage is developed in ANSYS and its resonant frequencies and deflections are also predicted to identify the effects of flexure hinges on overall performance.

Keywords: Planar positioning stage, Compliant parallel linkage, Electrostatic actuation, Flexure hinges, Finite element analysis.

1 Introduction

Precision manufacturing and metrology have been aided by the development of micro positioning stages. Micro positioning stages have been essential instruments in laser welding, lithography processes for semiconductors and thin-film transistor liquid crystal displays, probe and object positioning of atomic force microscopes (AFMs), scanning probe microscopes (SPMs), cell biology and medical research. Such practical demands have generated many studies in recent years. In general, a micropositioning stage is an instrument that positions an end-effector to a desired position in the workspace with sub-micrometer resolution. For superior resolution and accuracy, a micro positioning stage uses actuators, sensors and linkages that differ from those of conventional positioners. Piezoelectric stacks, thermomechanical actuators, electro-static combs, pressure-elongated cylinders and magnetostrictive materials are used as actuators for micro and nanopositioning. Capacitive proximity sensors, laser interferometers and linear variable differential transformers are used as sensors because of their high resolution. For micro/nano scale manipulation, several parallel manipulators employing compliant mechanisms have been designed. Flexure hinges in these mechanisms help in force and displacement transmission without wear and backlash. The number of degrees of freedom (DOFs) of a micropositioning stage is determined according to the use and purpose of the stage. Stages were originally limited to one or two DOFs (typically x and y). However, progress in the fields of micro manufacturing, biotechnology and optical measurements has increased the demand for more degrees of freedom and higher resolution.

U.Sudhakar
Department of Mechanical Engineering, CEC, Visakhapatnam, E-mail:mr.u.sudhakar@gmail.com

J.Srinivas (Corresponding author)
Department of Mechanical Engineering, NIT-Rourkela, E-mail: srin07@yahoo.co.in.

1.1 Literature review

Several authors reported various types of parallel kinematic linkages for the design of micropositioning stages. Chen *et al.* [1] reported the design of a planar compliant fixture, comprising a platform movable in X-Y-θ and three-flexure based supporting legs. Company *et al.* [2] presented a kinetostatic analysis of a planar parallel mechanism intended to be used in high accuracy applications. Liu *et al.* [3] illustrated the methodology of design, fabrication and testing of a micro electromechanical system-based three axis positioning stage. Mukhopadhyay *et al.*[4] presented design and analysis approach of a planar micropositioning stage having three degrees of freedom based on 3-PRR parallel kinematic linkage. Yong and Lu [5] employed 3-RRR parallel kinematic linkage with flexure hinges for development of a micromotion stage. Tian *et al.* [6] presented a five-bar compliant linkage working as micromanipulator driven with piezoelectric actuators and lever mechanism. Dong and Ferreira [7] presented the design and analysis of a cantilever device operated by a two degree of freedom translational micropositioning stage. Arbat *et al.* [8] shown the design and validation procedure of a control circuits for micro-cantilever tools of a robot. Li and Xu [9] described the modelling and evaluation of a nearly uncoupled XY micromanipulator designed for micro-positioning applications. Xu and Li [10] studied the factors affecting the positioning accuracy of an XY parallel micromanipulator operated with piezoelectric actuation. Moon *et al.* [11] developed a piezoelectrically actuated 6-degree of freedom stage for micropositioning. More recently, Majarena *et al.*[12] described algorithms for designing a two degree of freedom platform based on parallel kinematics for positioning and orienting two ultra precision cameras.

1.2 Objectives of the present work

Based on the available literature, it is found that piezoelectric actuation is more commonly used in micro positioning stages with compliant planar and spatial parallel linkages having flexure hinges. As a viable alternative, electrostatic actuation can also be used to generate narrow deformations and required resolution/sensitivity of the stage may be obtained. Present work deals with the description of micropositioning stage based on simple 3-RPR planar parallel linkage actuated with electrostatic comb-drives. In continuation of earlier work [13], it is proposed to define the singular-free configuration in workspace and the dynamic analysis is conducted to know the effects of narrow circular flexural hinges on the platform motion and natural frequencies of the system.

2 Kinematic Analysis

Conventional 3-RPR planar parallel linkage contains on each of its three limbs, two revolute passive joints with one active prismatic joint in-between forming the coordination and orientation of moving platform. The proposed compliant linkage uses flexural hinges to replace the revolute joints so as to minimize the loss of motion at the platform, while the prismatic drive is provided by electro static comb-drives. Figure 1 shows the architecture of proposed stage. It is a monolithic compliant structure. The flexure hinges in micropositioning applications are highly favored as precision kinematic elements due to their high repeatability and

continuous force/displacement transfer without the detrimental properties frequently found in mechanical linkages such as backlash, stick-slip and wear. However, the limited travel–range and weak strength confines their use.

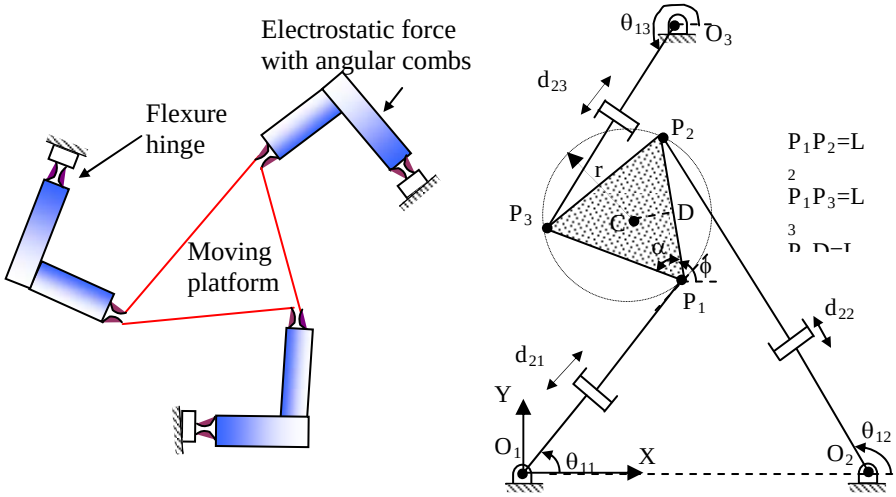

(a) Proposed micro mechanism (b) Conventional counterpart

Figure 1: 3-RPR parallel Linkage

Flexure hinges have a large rotational compliance along the sensitive axis but small compliances along the other axes. If one end of a flexure hinge is fixed and a lateral force is applied to the other end, the neck of flexure bends, resulting in a rotational motion of the other end. Two types of flexure hinges are commonly used: (i) 1-D and (ii) 2-D flexure hinges, based on their relative rotational degrees of freedom of one side with respect to the other. The first type of flexure hinges are widely used in micropositioning application since they can be easily constructed using wire electric discharge machining. An empirical formula describing the rotational stiffness for a 1-D flexure hinge as seen in Figure .2 is described by [14] $K_b = \frac{2Eht^{5/2}}{9\pi R^{1/2}}$ Nm/rad, where E is the Young's modulus and h, t and R are dimensions shown in Figure 2.

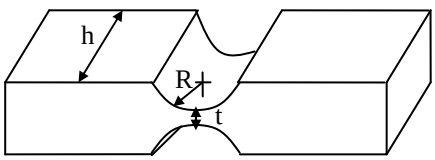

Figure 2: One-dimensional Flexure hinge with rectangular cross-section

This relation applies in the range t/R $\in$[0.05 0.5]. Dimensions of these flexure hinges and their positions on the links greatly influence the characteristics of the micro/nano

manipulation mechanism, especially its working range. Referring to Fig. 1(b), the position kinematics of conventional 3-RPR linkage is represented as follows:
Length of ith limb d_{2i}, (which is the distance between points flexure hinge centres O_i and P_i) is given by:

$$d_{2i}^2=(P_{ix} -O_{ix})^2 + (P_{iy} - O_{iy})^2, \quad i=1,2,3. \tag{1}$$

In line with Fig.1(b), for each leg with the coordinates of the base triangle shown, we can write:

$$d_{21}^2=x^2 + y^2$$
$$d_{22}^2=(x - x_{O2}+L_2\cos\phi)^2 + (y +L_2\sin\phi)^2$$
$$d_{23}^2=(x- x_{O3}+L_3\cos(\phi+\alpha))^2 + (y- y_{O3}+L_3\sin(\phi+\alpha))^2 \tag{2}$$

where $x(=x_C- L_x \cos\phi+L_y \sin\phi)$ and $y(=y_C- L_x \sin\phi - L_y \cos\phi)$ are the coordinates of one the points (P_1) on the moving platform (triangle) and L_x, L_y are the horizontal and vertical distances of platform center C with respect to coordinate frame at P_1. Often for symmetric analysis, fixed and movable platforms are treated as equilateral triangles ($\alpha=\pi/3$), so that the parameters L_x, L_y, L_2 and L_3 are expressed in terms of the radius of circumscribed circle r, while r_1 is used to represent radius of circle circumscribing base triangle. In present case, $L_x=r\cos(\alpha/2)$ and $L_y=r\sin(\alpha/2)$. Also $L_2=L_3=2L_x$. Workspace through which the stage can displace depends on the deflection of the mechanism under the actuation force provided by comb drive actuators. It is determined by using a computer search algorithm over a candidate region in which it resides. The workspace circles defined by Eqs.(2) are used to determine workspace based on the minimal and maximal values of d_{2i} (i=1,2,3).Velocity equation that relates the joint rates $\{\dot{q}\}$ and velocity vector of table-center $\{\dot{X}_C\}$ is written by differentiating the position equation (2) as:

$$[J_q]\{\dot{q}\} =[J_X]\{\dot{X}_C\} \tag{3}$$

where $[J_q]$ and $[J_X]$ are Jacobian matrices. The composite matrix $[J]=[J_q]^{-1}[[J_X]$ defines the Jacobian of the manipulator system, which in general should be of full rank. In singular configurations only it becomes rank deficient. For the present case, the following matrices are used:

$$[J_q]=\begin{bmatrix} d_{21} & 0 & 0 \\ 0 & d_{22} & 0 \\ 0 & 0 & d_{23} \end{bmatrix} \tag{4}$$

$$[J_X]=\begin{bmatrix} x & y & 0 \\ (x-x_{O2})+L_2\cos\phi & y+L_2\sin\phi & L_2(y\cos\phi-(x-x_{O2})\sin\phi) \\ (x-x_{O3})+L_3\cos(\phi+\alpha) & (y-y_{O3})+L_3\sin(\phi+\alpha) & L_3((y-y_{O3})\cos(\phi+\alpha)-(x-x_{O3})\sin(\phi+\alpha)) \end{bmatrix} \tag{5}$$

A numerical approach is adopted for identification of singularities based on the performance index known as condition number. The condition number expresses how a relative error in joint coordinates gets multiplied and leads to a relative error at the moving platform. It characterizes in some sense the dexterity of the robot and is defines as:

$$\kappa = \left\|[J]^{-1}\right\|\left\|[J]\right\| \tag{6}$$

where the Euclidean norm $\|.\|$ of a matrix [J] is given by

$$\|J\| = \sqrt{\mathrm{tr}([J]^T[W][J])} \tag{7}$$

Here, $[W]=\frac{1}{3}[I]$ for the purpose of normalization, with [I] as 3×3 identity matrix. The condition number κ is a function of geometrical parameters as well as configuration variables [15] and varies from 1 to ∞. When the condition number is ∞, it refers to the singular configuration, while κ=1 indicates the condition of isotropic dexterity. Thus, objective is to maximize the global dexterity index defined as $GDI=\frac{1}{V}\int(1/\kappa)dV$, where V represents the workspace volume. Figure 3 shows the maximum reachable position workspace for the dimensions under consideration using the method direct search [16]. The larger circles represent the regions covered independently by each limb with maximum stroke of prismatic joint. In practice, the maximum rotation angle of flexure hinges is determined by the allowable stress of material and is examined using finite element analysis.

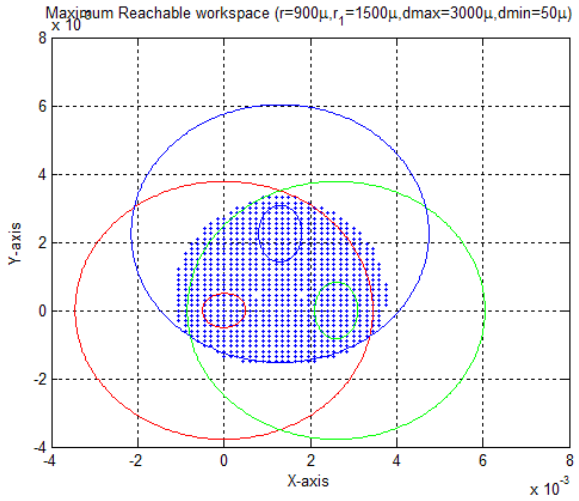

Figure 3: Maximum reachable workspace (units of X and Y axes are in m)

Figure 4 shows the singularities identified in the workspace based on the condition number. Here, whenever the value of GDI becomes less than 1×10^{-20}, the state is recorded as singular. The important dimensions like radii of the movable and fixed platforms: r and r_1, the extreme values d_{2imin} and d_{2imax} are arrived. Of the 15255 points in reachable workspace vicinity, only 30 points (marked as red) are found to be singular.

3 Static and Dynamic Analysis

A pseudo-rigid body model simplifies the static problem of mechanisms with flexure hinges. Approach is to separate the links and apply reaction forces on them. Based on the equilibrium, the equations of the links are established. The linear comb drive

actuator generates a force F_{comb} under the actuation voltage V to deflect the hinges so that the mechanism displaces in the workspace. This force is given by [4]:

$$F_i = n\frac{b\varepsilon_0 V^2}{\delta} \qquad (i=1,2,3) \qquad (8)$$

where n is number of comb fingers (=235), ε_0 is permittivity of free space (8.854×10^{-12} F/m), b is width of the finger (=50 μm) and δ (=3 μm) is gap between two neighbouring fingers. With these dimensions, when actuation voltage is 90 volts, the drive provides a force equal to 280.9 μN.

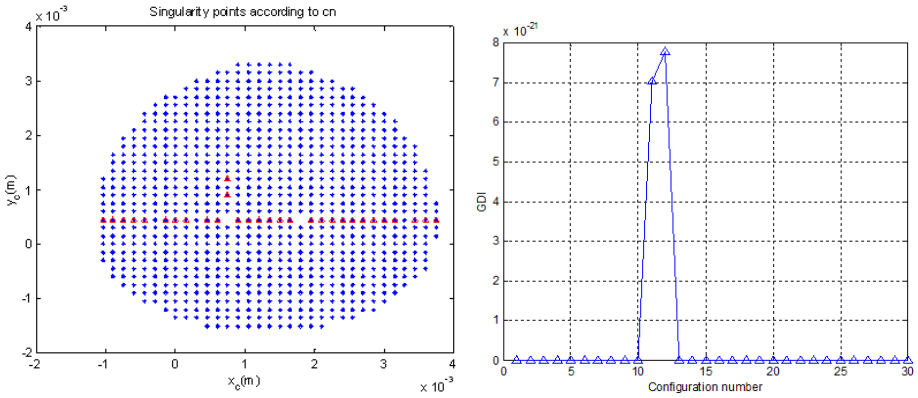

Figure 4: Singularities (in red) based on condition number

In the proposed linkage, when comb drives are actuated, the work done by them must be balanced by the energy stored at the hinges. Since there are two hinges in each limb, we can write from principle of virtual work:

$$F_1\Delta d_{21} + F_2\Delta d_{22} + F_3\Delta d_{23} = 2(\tfrac{1}{2} K_b \theta_{11}^2 + \tfrac{1}{2} K_b \theta_{12}^2 + \tfrac{1}{2} K_b \theta_{13}^2) \qquad (9)$$

Thus, by writing θ_{11}, θ_{12} and θ_{13} in terms of translations of prismatic links Δd_{21}, Δd_{22} and Δd_{23}, we can estimate the slider displacement and hence the table motion for a known applied voltage. This can be written as: $\Delta\tau = J^{-1}\Delta d$ and defines resolution of the linkage in terms of resolution of the comb-drive actuators. Resolution is considered constant in small working range. A finite element model of the proposed mechanism is developed in ANSYS with the joint stiffness modelled as a torsional spring. The electrostatic forces are applied at the connecting legs, so as to measure the displacements and stresses in the system. The links of this model use BEAM188 elements with realistic parameters so that it accounts deflection of hinges and links, while the moving platform is modelled by using PLANE183 elements (8 node 2 DOF plate) as shown in Figure 5.The flexure hinges are modelled using COMBIN14 with torsional rotation option. As PLANE183 cannot model the rotational constraints at the corners where the links join with moving platform, the corner nodes are also joined by BEAM188 elements. The dimensions of the hinges (given as scalar parameters) are: width h=70 μm, radius at the neck R=300 μm and neck thickness t=12 μm and E=131 GPa and yield stress of silicon material=7000 MPa. The displacements of the table centre driven by one of the three actuators are obtained and shown in Figure 6. The relationship between the actuation and Cartesian space is therefore linear. Using ANSYS, the Jacobian matrix can be determined as follows:

each input link is displaced by Δd_2 while other two links are constrained to have zero displacement; then the moving platform displacement and rotation are recorded. Using the results from three displacement cases, the Jacobian can be filled one column at a time. Natural frequencies and the dynamic behaviour of a micro positioning stage is crucial aspect for its successful operation in manufacture. The stage should respond quickly to fast changes in the commanded position but needs to be robust at the same time.

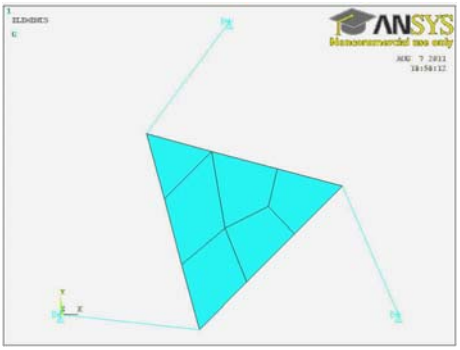

Figure 5 ANSYS image of the model

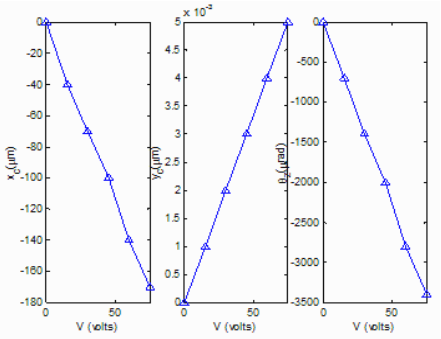

Figure 6 Displacements of platform

Reduced mode extraction method is used to carry-out modal analysis. Table 1 reports the first three natural frequencies of the stage as a function of flexure hinge parameter t/R.

Table 1 Natural Frequencies of the stage (in Hz)

t/R	Mode-1	Mode-2	Mode-3
0.08	693	693	1662
0.10	764	764	1727
0.25	821	821	1855
0.40	848	848	1933

These modes correspond to the two translations and a rotational motion. Both translation (first two) modes occur at same frequencies due to symmetry of linkage. As thickness of hinge reduces for a given value of R, all the frequencies dropped down considerably indicating the effect of hinge-flexure on the system dynamics.

4 Conclusion

This work presented numerical analysis of X-Y-θ micro-positioning stage based on planar 3-RPR parallel mechanism. A pseudo-rigid body model that considers the flexure hinges (instead of revolute joints as in conventional linkage) as equivalent torsional springs was employed to analyze the motion of compliant parallel mechanism. Inverse kinematics, workspace and singularity analysis were carried out as in conventional parallel linkages. The idea of electrostatic actuation for driving the prismatic links in 3-RPR compliance linkage has been proposed. The natural frequencies of the system were obtained as a function of flexure joint parameters. As

a future scope of this work, the stage has to be fabricated and the workspace characteristics and resolution need to be correctly predicted.

References

[1] W.J.Chen, W.Lin, K.H.Low and G.Yang, "A 3-DOF flexure-based fixture for passive assembly of optical switches", Proc. IEEE/ASME Int. Conf. Advanced Int. Mechatronics, Monterey, USA, July 2005, pp.618-623.

[2] O.Company, S.Krut and F.Peirrot, "Analysis of a high resolution planar PKM", Proc.12th IFToMM World congress, Besancon, June 2007, pp.1-6.

[3] X.Liu, K.Kim and Y.Sun, "A MEMS stage for 3-axis nanopositioning", J.Micromechanics & Microengg., vol.17, pp.1796-1802, 2007.

[4] D.Mukhopadhyay, J.Dong, E.Pengwang, P.Ferreira, "A SOI-based planar parallel kinematics nanopositioning stage", Sensors and Actuators A:Physical, vol.147, pp.340-351, 2008.

[5] Y.K.Yong and T.F.Lu, "Kinetostatic modeling of 3-RRR compliant micro-motion stages with flexure hinges", Mechanisms and Machine theory, vol.44, pp.1156-1175, 2009.

[6] Y.Tian, B.Shirinzadeh, D.Zhan, X.Liu and D.Chetwynd, "Design and forward kinematics of a compliant micro-manipulator with lever mechanism", Precision Engineering, vol.33, pp.466-475, 2009.

[7] J.Dong and P.M.Ferreira, "Electrostatically Actuated Cantilever with SOI-MEMS Parallel Kinematic XY Stage", IEEE Journal of Microelectromechanical Systems, vol.18, 641-651, 2009.

[8] A.Arbat, E.Edquist, R.Casanova, J.Brufau J.Sanitier, S.Johansson and A.Dieguez, "Design and validation of control circuits for a micro-cantilever tool of a micro robot", Sensors & Actuators A, vol.153, pp.1324-1329, 2009.

[9] Y.Li and Q.Xu, "Modeling and performance evaluation of a flexure-based XY parallel micromanipulator", Mechanism and Machine Theory, Vol.44, pp.2127-2152, 2009.

[10] Q.Xu and Y.Li, "Dahl model-based hysteresis compensation and precise positioning control of an X-Y parallel micromanipulator with piezoelectric actuation", J. Dynamic System, Measurements and Control, Trans.ASME, vol..132, pp.041011-1-12, 2010.

[11] J.H.Moon, H.J.Pahk and B.G.Lee, "Design, modelling and testing of a novel 6-DOF micropositioning stage with low profile and low parasitic motion", Int.J.Adv.Manuf.Technology, vol.55, pp.163-176, 2011.

[12] A.C.Majarena,J.Santolana, D.Samper and J.J.A.Martin, "Spatial resolution-based kinematic design of a parallel positioning platform", Int.J. Adv.Man.Tech., vol.53, pp.1149-1165, 2011.

[13] U.Sudhakar and J.Srinivas, "Kinematics of 3-RPR planar parallel micro-positioning stage", Proc. National Symposium on Planar Parallel Robots and Mechanisms, Jan.2010, Bhilai, India, pp.7-14.

[14] J.M.Paros and L.Weisbord, "How to design flexure hinge", Mach.Design, vol.37,pp.151-156, 1965.

[15] L.W.Tsai. *Robot Analysis: the mechanics of serial and parallel manipulators* NY: John Wiley & Sons, 1999.

[16] M.Z.Huang and J.L.Thebert, “A study of workspace and singularity characteristics for design of 3-DOF planar parallel robots”, Int. J. Adv. Man. Tech., vol.51, pp.789-797, 2010.